



Description of *Trichotokara nothriae* n. gen. et sp. (Apicomplexa, Lecudinidae) – An intestinal gregarine of *Nothria conchylega* (Polychaeta, Onuphidae)

Sonja Rueckert*, Brian S. Leander

Canadian Institute for Advanced Research, Program in Integrated Microbial Biodiversity, Departments of Botany and Zoology, University of British Columbia, #3529 – 6270 University Blvd., Vancouver, BC, Canada V6T 1Z4

ARTICLE INFO

Article history:

Received 12 November 2009

Accepted 11 March 2010

Available online 23 March 2010

Keywords:

Alveolata

Apicomplexa

Lecudinidae

Lecudina

Parasite

Phylogeny

Polychaeta

Trichotokara nothriae

ABSTRACT

The trophozoites of a novel gregarine apicomplexan, *Trichotokara nothriae* n. gen. et sp., were isolated and characterized from the intestines of the onuphid tubeworm *Nothria conchylega* (Polychaeta), collected at 20 m depth from the North-eastern Pacific Coast. The trophozoites were 50–155 μm long with a mid-cell indentation that formed two prominent bulges (anterior bulge, 14–48 μm wide; posterior bulge, 15–55 μm wide). Scanning electron microscopy (SEM) demonstrated that approximately 400 densely packed, longitudinal epicytic folds (5 folds/ μm) inscribe the surface of the trophozoites, and a prominently elongated mucron (14–60 μm long and 6–12 μm wide) was covered with hair-like projections (mean length, 1.97 μm ; mean width, 0.2 μm at the base). Although a septum occurred at the junction between the cell proper and the mucron in most trophozoites, light microscopy (LM) demonstrated that the cell proper extended into the core of the mucron as a thin prolongation. A spherical nucleus (8–20 μm) was situated in the middle of the trophozoites, and gamonts underwent caudal syzygy. The small subunit (SSU) rDNA sequence and molecular phylogenetic position of *T. nothriae* was also characterized. The sequence from this species was the most divergent of all SSU rDNA sequences currently known from gregarines and formed a weakly supported clade with *Lecudina polymorpha*, which also possesses densely packed epicytic folds (3–5 folds/ μm) and a prominently elongated mucron.

© 2010 Elsevier Inc. All rights reserved.

1. Introduction

Apicomplexans form a diverse group of unicellular parasites containing about 6000 described species and approximately 1.2–10 million undescribed species (Hausmann et al., 2003; Adl et al., 2007; Morrison, 2009). There are four major groups of apicomplexans recognized: (eu)coccidians, haemosporidians, piroplasmids and gregarines (Adl et al., 2005). Because some of these groups include pathogens of humans and life stock (e.g., *Plasmodium* – the causative agent of malaria), these species are better studied than groups that have no known medical or economic impact. Among the least understood apicomplexan parasites are gregarines, especially those inhabiting the oceans. Marine gregarines are dynamic extracellular parasites that inhabit the intestines and coeloms of invertebrates, and improved knowledge of these lineages will help elucidate the overall diversity and early evolutionary history of apicomplexans as a whole (Leander, 2008).

Gregarines have been conveniently lumped into three groups: archigregarines, eugregarines, and neogregarines (Grassé, 1953).

The vast majority of described gregarine species are considered eugregarines, and, in large part, this is due to the fact that many eugregarines infect insects, which have garnered more attention from the parasitological community. Eugregarines, however, also occur in marine and freshwater habitats and have intestinal trophozoites (relatively large feeding stages) that are significantly different in morphology and behaviour from that of the infective sporozoites. Most eugregarine species that inhabit marine invertebrates have been classified within a poorly circumscribed family called the Lecudinidae Kamm, 1922 (25 genera) and within the genus *Lecudina* Mingazzini, 1899 (Levine, 1988). This genus has emerged as a “catch-all” taxon for marine aseptate gregarines that inhabit the intestines of polychaetes (and a few other host taxa). Consequently, the actual diversity of these parasites is greatly underestimated, and the identity and composition of *Lecudina* has become even more ill-defined within the context of modern molecular phylogenetic and comparative ultrastructural data (Leander et al., 2003b; Leander, 2008; Rueckert and Leander, 2009).

New species (i.e., morphotypes or phylotypes) of gregarines are generally discovered in previously unexplored host species, and closely related host species tend to be infected by closely related gregarine species (e.g., Levine, 1979; Perkins et al., 2000; Landers and Leander, 2005; Rueckert and Leander, 2008, 2009; Simdyanov,

* Corresponding author. Address: Departments of Botany and Zoology, University of British Columbia, #3529 – 6270 University Blvd., Vancouver, BC, Canada V6T 1Z4. Fax: +1 604 822 6089.

E-mail address: rueckert@interchange.ubc.ca (S. Rueckert).

2009). Accordingly, the host taxon has been used as corroborating evidence for the delimitation of different gregarine species that are otherwise differentiated on the basis of molecular phylogenetic data and comparative morphology. A common morphological feature of the trophozoites of marine eugregarines is a cell cortex consisting of longitudinal epicytic folds that can vary considerably in overall number (Leander et al., 2003b; Leander, 2008). Some marine gregarines also possess conspicuous hair-like projections on the surface of the trophozoites, such as *Filipodium* (archigregarine), *Diplauxis* (eugregarine), *Urospora* (eugregarine) and *Cochleomeritus* (eugregarine). The hair-like projections in *Filipodium*, *Diplauxis* and *Urospora* cover the entire trophozoite surface (Hoshide and Todd, 1996; Dyakin and Simdyanov, 2005; Prensier et al., 2008; Rueckert and Leander, 2009), whereas the hair-like projections of *Cochleomeritus* are limited to the attachment apparatus, called the mucron (Levine, 1973). In each case, the longitudinal epicytic folds and hair-like projections are inferred to increase surface area, presumably for the acquisition of nutrients within the intestinal lumen of the host.

In this study, we describe a novel marine eugregarine with a prominent elongated mucron covered with hair-like projections: *Trichotokara nothriae* n. gen. et sp. This species was isolated from the intestines of *Nothria conchylega*, a tube-forming polychaete (Onuphidae) collected from the North-eastern Pacific Ocean. We characterized the morphological features of the trophozoites in this novel species with light and scanning electron microscopy (LM and SEM, respectively) and established a DNA signature (i.e., barcode) for the new lineage by generating its small subunit (SSU) rDNA sequence. Molecular phylogenetic analyses of the new sequence from *T. nothriae* also enabled us to re-evaluate and discuss the systematics of *Lecudina polymorpha*, another gregarine with a prominent elongated mucron.

2. Materials and methods

2.1. Collection and isolation of organisms

A dredge haul was conducted at Wizard Islet (48°51'6"N, 125°09'4"W) in June 2008 and June 2009 at a depth of 20 m during two trips on the research vessel MV/Alta from the Bamfield Marine Science Centre, British Columbia, Canada. Tubes of the onuphid polychaete *N. conchylega* (Sars, 1835) were collected from these samples.

The intestines of the host organism were dissected with fine-tipped forceps under a low magnification stereomicroscope (Leica MZ6) in order to extract the trophozoites of *T. nothriae*. Gut contents containing trophozoites were examined with an inverted compound microscope (Zeiss Axiovert 200 or Leica DM IL), and individual trophozoites were isolated by micromanipulation. Before being prepared for microscopy and DNA extraction, individual trophozoites were washed three times in filtered and autoclaved seawater.

2.2. Light and scanning electron microscopy

Differential interference contrast (DIC) light micrographs of the trophozoites of *T. nothriae* were taken with a compound microscope (Zeiss Axioplan 2) connected to a colour digital camera (Leica DC500). Individual trophozoites of *T. nothriae* ($n = 21$) were prepared for scanning electron microscopy (SEM) using the OsO₄ vapour protocol described previously (Rueckert and Leander, 2008, 2009). Isolated cells were deposited directly into the threaded hole of a Swinnex filter holder, containing a 5 µm polycarbonate membrane filter (Millipore Corp., Billerica, MA), that was submerged in 10 ml of seawater within a small canister (2 cm diameter and

3.5 cm tall). A piece of Whatman filter paper was mounted on the inside base of a beaker (4 cm dia. and 5 cm tall) that was slightly larger than the canister. The Whatman filter paper was saturated with 4% OsO₄ and the beaker was turned over the canister. The parasites were fixed by OsO₄ vapours for 30 min. Ten drops of 4% OsO₄ were added directly to the seawater and the parasites were fixed for an additional 30 min on ice. A 10 ml syringe filled with distilled water was screwed to the Swinnex filter holder and the entire apparatus was removed from the canister containing seawater and fixative. The parasites were washed then dehydrated with a graded series of ethyl alcohol and critical point dried with CO₂. Filters were mounted on stubs, sputter-coated with 5 nm gold, and viewed under a scanning electron microscope (Hitachi S4700). Some SEM data were presented on a black background using Adobe Photoshop 6.0 (Adobe Systems, San Jose, CA).

2.3. DNA isolation, PCR amplification, cloning, and sequencing

DNA was extracted from two different isolates of trophozoites collected at different times. Seventeen individual trophozoites (isolate 1) and 18 individual trophozoites (isolate 2) were manually isolated from dissected hosts, washed three times in filtered and autoclaved seawater, and deposited into a 1.5 ml Eppendorf tube. Genomic DNA was extracted from the cells using the MasterPure complete DNA and RNA purification Kit (EPICENTRE, Madison, WI, USA). Small subunit rDNA sequences were PCR amplified using puReTaq Ready-to-go PCR beads (GE Healthcare, Quebec, Canada) and the following eukaryotic PCR primers: F1 5'-GCGCTACCTGGTTGATCCTGCC-3' and R1 5'-GATCCTTCTGCAGGTTCACTAC-3' (Leander et al., 2003a). The following internal primers, designed to match existing eukaryotic SSU sequences, were used for nested PCR: F2 5'-AAGTCTGGTGCCAGCAGCC-3', F3 5'-TGCGTACCTGGTTGATCC-3' and R2 5'-GCCTYGCACCATACTCC-3'. PCR products corresponding to the expected size (~1806 bp) were gel isolated and cloned into the pCR 2.1 vector using the TOPO TA cloning kit (Invitrogen, Frederick, MD). Eight cloned plasmids, for each PCR product, were digested with *EcoRI*, and inserts were screened for size using gel electrophoresis. Two identical clones were sequenced with ABI Big-dye reaction mix using vector primers and internal primers oriented in both directions. The SSU rDNA sequences were identified by BLAST analysis and molecular phylogenetic analyses (GenBank Accession number GU592817).

2.4. Molecular phylogenetic analysis

The new SSU rDNA sequence from *T. nothriae* was incorporated into two alignments using MacClade 4 (Maddison and Maddison, 2000) and visual fine-tuning: (1) a 42-sequence alignment representing all major groups of eukaryotes and (2) a 64-sequence alignment representing the diversity of gregarines. The 42-sequence alignment enabled us to more confidently establish the relationship of the highly divergent sequence from *T. nothriae* with gregarine apicomplexans (Supplementary file). The 64-sequence alignment enabled us to more thoroughly establish the relationship of *T. nothriae* within gregarine apicomplexans. The program PhyML (Guindon and Gascuel, 2003; Guindon et al., 2005) was used to analyze the 42-sequence alignment (928 unambiguously aligned positions; gaps excluded) and the 64-sequence alignment (1019 unambiguously aligned positions; gaps excluded) with maximum-likelihood (ML) using a general-time reversible (GTR) model (Posada and Crandall, 1998) incorporating the fraction of invariable sites and a discrete gamma-distribution with eight rate categories (GTR + I + Γ + 8 model: $\alpha = 0.450$ and $I = 0.068$ for the 64-sequence alignment; $\alpha = 0.371$ and $I = 0.000$ for the 42-sequence alignment). ML bootstrap analyses were performed on 100 re-sam-

pled datasets using the same program and the same GTR + I + Γ + 8 model.

Bayesian analysis of both alignments was performed using the program MrBayes 3.0 (Huelsenbeck and Ronquist, 2001). The program was set to operate with GTR, a gamma-distribution, and four Monte Carlo Markov chains (MCMC; default temperature = 0.2). A total of 2,000,000 generations were calculated with trees sampled every 50 generations and with a prior burn-in of 100,000 generations (2000 sampled trees were discarded; burn-in/convergence was checked manually). A majority rule consensus tree was constructed from 38,001 post-burn-in trees. Posterior probabilities correspond to the frequency at which a given node was found in the post-burn-in trees. Independent Bayesian runs on each alignment yielded the same results.

2.5. GenBank accession numbers

(AF494059) *Adelina bambarooniae*, (FJ459737) *Amoebogregarina nigra*, (AJ415519) *Amoebophrya* sp. ex. *Prorocentrum micans*, (DQ462456) *Ascogregarina culicis*, (DQ462455) *Ascogregarina taiwanensis*, (AY603402) *Babesia bigemina*, (L19068) *Cryptosporidium baileyi*, (AF093489) *Cryptosporidium parvum*, (AF093502) *Cryptosporidium serpentis*, (AF39993) *Cytauxzoon felis*, (U67121) *Eimeria tenella*, (AB191437, AF372779, AF372780, AY179975, AY179976, AY179977, AY179988) Environmental sequences, (FJ832163) *Filipodium phascolosomae*, (FJ459741) *Gregarina blattarum*, (FJ459743) *Gregarina coronata*, (FJ459746) *Gregarina kingi*, (AF129882) *Gregarina niphandrodes*, (FJ459748) *Gregarina polymorpha*, (FJ832159) Gregarine from *Paranemertes peregrina*, (FJ832156) Gregarine from *Phyllochaetopterus prolifica*, (FJ832160) Gregarine from *Tubulanus polymorpha*, (AF022194) *Gymnodinium fuscum*, (AF286023) *Hematodinium* sp., (AF130361) *Hepatozoon catesbiana*, (FJ459750) *Hoplorhynchus acanthatholius*, (DQ093796) *Lankesteria abbotti*, (EU670240) *Lankesteria chelyosomae*, (EU670241) *Lankesteria cystodytae*, (AF080611) *Lankesterella minima*, (FJ832157) *Lecudina longissima*, (AY196706) *Lecudina polymorpha* morphotype 1, (AY196707) *Lecudina polymorpha* morphotype 2, (AF457128) *Lecudina tuzetae*, (FJ459753) *Leidyana haasi*, (AF457130) *Leidyana migrator*, (DQ093795) *Lithocystis* sp., (AB000912) Marine parasite from *Tridacna crocea*, (AY334568) *Mattesia geminata*, (AF457127) *Monocystis agilis*, (AJ271354) *Neospora caninum*, (AF129883) *Ophryocystis elektroscirrha*, (FJ459755) *Paraschneideria metamorphosa*, (AY196708) *Platyproteum vivax* ex. *Selenidium vivax*, (FJ459756) *Prismatospora evansi*, (FJ459757) *Protomagalhaensia granulosa*, (DQ093794) *Pterospora floridiensis*, (DQ093793) *Pterospora schizosoma*, (GQ149767) *Rhytidocystis cyamus*, (DQ273988) *Rhytidocystis polygordiae*, (M64244) *Sarcocystis muris*, (FJ832161) *Selenidium orientale*, (FJ832162) *Selenidium pisinus*, (DQ683562) *Selenidium serpulae*, (AY196709) *Selenidium terebellae*, (DQ176427) *Syncystis mirabilis*, (AF013418) *Theileria parva*, (M97703) *Toxoplasma gondii* and (GU592817) *Trichotokara nothriae* n. gen. et sp.

3. Results

3.1. Morphology of *T. nothriae* n. gen. et sp.

The trophozoites of *T. nothriae* were approximately 93 μm long (50–155 μm , $n = 23$) and displayed the shape of a guitar under the light microscope (Fig. 1a–e). SEM examination of the trophozoites demonstrated that the cells were round in transverse section rather than flattened (Fig. 2a). Trophozoites were rigid and gliding motility was not observed. The trophozoites could be divided into two parts: the cell body proper and a prominently elongated mucron (Fig. 1a). The cell body proper was indented forming two bulges, one at the anterior end and one at the posterior end of

the cell (Fig. 1a and d). The anterior bulge measured 28 (14–48) μm wide; the posterior bulge measured 30 (15–55) μm wide. The posterior end was rounded to pointed (Figs. 1a and d, 2a), while the anterior end tapered into a neck-like constriction near the base of the elongated mucron. In some cases, the mucron was of approximately the same length as the cell body proper, about 31 μm long (14–60 μm , $n = 24$) and 10 μm (6–12 μm , $n = 24$) wide, and was covered with hair-like projections (Fig. 2a and b). A vacuole was visible at the anterior end of the mucron in some individuals of *T. nothriae* (Fig. 1a and c). In most trophozoites, a distinct septum occurred at the junction between the cell body proper and the mucron (Fig. 1a and c); however, some trophozoites lacked the mucron completely. The cell body proper formed the core of the mucron via a thin prolongation (Fig. 1d–f). A spherical nucleus that measured 12 (8–20) μm in diameter ($n = 19$) was mostly situated in the middle of the cell body proper or slightly shifted to the anterior or posterior end. A nucleolus that measured 4 μm in diameter was observed in one trophozoite. The cytoplasm had a granular appearance. Gamonts without elongated mucrons were observed in caudal syzygy (Fig. 1f). Neither sporozoites nor oocysts were observed.

Scanning electron micrographs demonstrated the three-dimensional cell shape of the trophozoite (Fig. 2a). The trophozoite body surface was inscribed with approximately 400 densely packed longitudinal epicytic folds (5 folds/ μm) (Fig. 2a). Some epicytic folds merged together (Fig. 2c). The mucron lacked folds and was covered with hair-like projections with a mean length of 1.97 μm (0.77–4.3 μm , $n = 11$) and a mean width of 0.2 μm (0.18–0.23 μm , $n = 11$) at the base (Fig. 2b). The hair-like projections were protrusions from the underlying cortex (Fig. 2b). The junction between the cell body proper and the mucron was obscured by over-arching hair-like projections under the SEM (Fig. 2c).

3.2. Molecular phylogenetic analyses

Phylogenetic analyses of the 64-taxon data set resulted in a strongly supported clade of dinoflagellates (outgroup) and a poorly resolved backbone for the apicomplexan ingroup (Fig. 3). The apicomplexan backbone gave rise to: (1) a clade consisting of a paraphyletic group of coccidians and a strongly supported subclade of piroplasmids; (2) a rhytidocystid clade; (3) a cryptosporidian clade; (4) a moderately supported “terrestrial gregarine clade 1”, consisting of neogregarines, monocystid eugregarines and several eugregarines from insects, and (5) a strongly supported “terrestrial gregarine clade 2”, consisting of several eugregarines from insects. The sequences from marine archigregarines (e.g., *Selenidium*, *Platyproteum*, and *Filipodium*) formed several different lineages that branched independently from the apicomplexan backbone (Fig. 3). Marine eugregarines formed two sister clades: (1) a strongly supported clade consisting of urosporids (*Pterospora* and *Lithocystis*) and lecudinids (*Difficilina*, *Lankesteria* and *Lecudina*) and (2) a weakly supported clade consisting of *T. nothriae* n. gen. et sp. and two morphotypes of *L. polymorpha*.

The SSU rDNA sequences derived from the two independent isolates of *T. nothriae* were more divergent than any other gregarine sequence characterized so far. Accordingly, in order to further ensure that the highly divergent SSU rDNA sequence from *T. nothriae* was indeed from the new gregarine species, rather than a contaminant, we also analysed a 42-taxon alignment containing representatives of all major groups of eukaryotes. In this analysis, the sequence from *T. nothriae* clustered within a clade of alveolates (i.e., ciliates, perkinsids, dinoflagellates and apicomplexans) and specifically with other gregarine sequences, albeit with weak statistical support (Supplementary file).

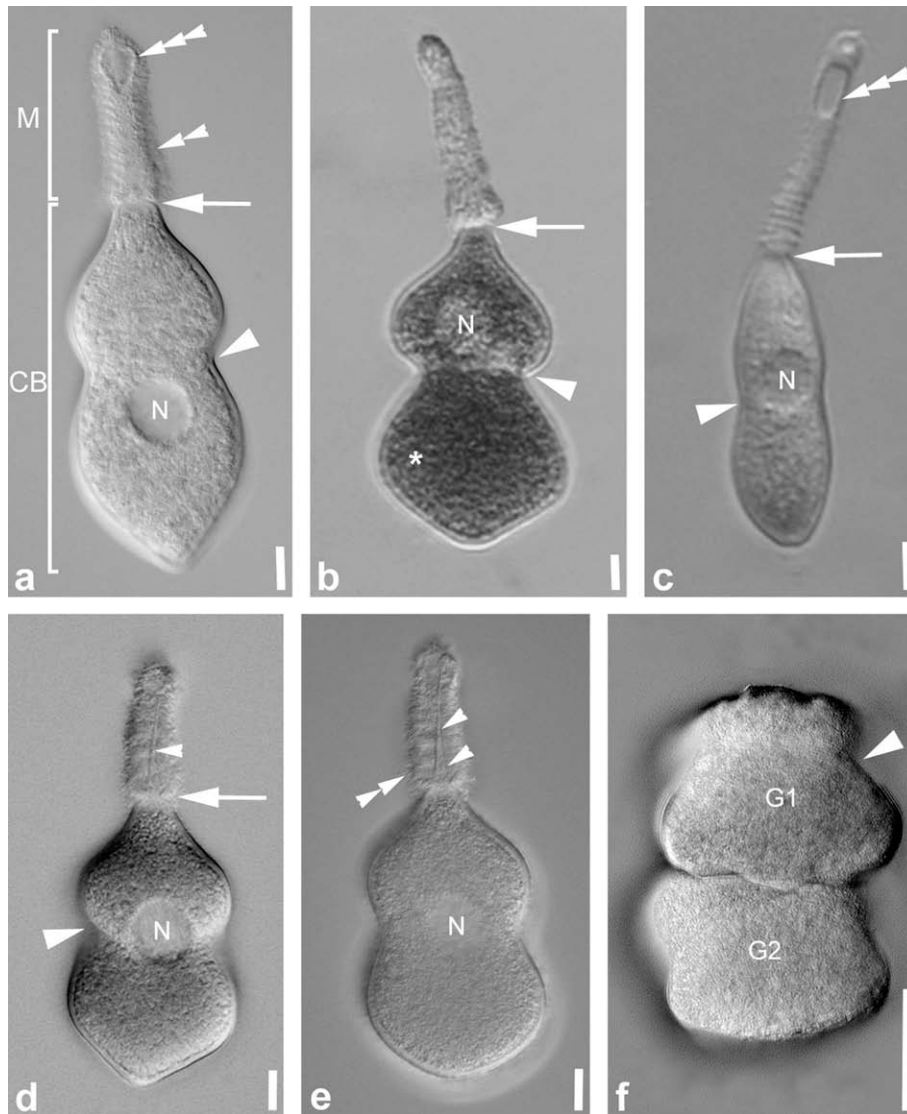


Fig. 1. Differential interference contrast (DIC) micrographs showing the general trophozoite morphology of *Trichotokara nothriae* n. gen. et sp. (a–c) Different individual trophozoites showing morphological variability. The trophozoite can be divided into an elongated mucron (M) and the cell body proper (CB). The traverse indentation (arrowhead) in the middle of the trophozoite gives the cell a guitar-like shape. The elongated mucron is covered with hair-like projections (double arrowhead) and is separated from the cell body proper by a junction (arrow). A vacuole (triple arrowhead) is visible at the anterior end of the mucron in some trophozoites. A spherical nucleus (N) is situated in the middle of the cell or shifted to the anterior or posterior end. The cell body proper is filled with granular cytoplasm (asterisk). (d) Another trophozoite showing the three-dimensional body with indentation (arrowhead) and the junction (arrow) between the cell body proper and the mucron. A thin prolongation (arrowhead) forms the core of the mucron. (e) The prolongation (arrowheads) inside the mucron stems from the cell body proper. The mucron is covered with hair-like projections (double arrowhead). (f) Two gamonts (G1 and G2) in caudal syzygy. In one gamont (G1) the indentation (arrowhead) is still visible. Scale bars: a–e = 10 μ m; f = 25 μ m.

4. Discussion

The Lecudinidae consists of about 25 genera, and most of the described species fall within the genus *Lecudina* (Levine, 1976). *Pontesia*, *Cochleomeritus* and *Diplauxis* are genera within the family known to possess hair-like projections on the trophozoites that are reminiscent of the hair-like projections described here for *T. nothriae* (Levine, 1977). Similar hair-like projections have also been described in genera of gregarines that fall outside of the Lecudinidae, such as *Filipodium* (Hoshide and Todd, 1996; Rueckert and Leander, 2009), *Urospora* (Dyakin and Simdyanov, 2005) and *Diplauxis* (Prensier et al., 2008), and in parasitic dinoflagellates, such as *Haplozoon* (Leander et al., 2002; Rueckert and Leander, 2008). Nonetheless, unlike most of these parasites, the trophozoites of *T. nothriae* possess hair-like projections that are restricted to an elongated mucron rather than over the entire cell surface (Fig. 2). The

only other described species of marine eugregarines with hair-like projections that are restricted to the mucron fall within the genus *Cochleomeritus* (Levine, 1973), which contains two species: *Cochleomeritus emersoni* Levine (1973) and the type species *Cochleomeritus lysidice* Hoshide (1944). Like *T. nothriae*, these two species infect onuphid polychaetes (*Diopatra ornata* Moore, 1911 and *Lysidice punctata* Grube, 1855).

Although their presence in onuphid polychaetes and possession of similar hair-like projections suggest that *C. emersoni*, *C. lysidice*, and *T. nothriae* are closely related to one another, the morphology of *T. nothriae* differs from *Cochleomeritus* in several significant ways (Table 1).

For instance, the two species of *Cochleomeritus* have much larger trophozoites (*C. lysidice* 450 \times 175 μ m and *C. emersoni* 525 \times 150 μ m) that are substantially different in overall cell shape than those observed in *T. nothriae* (the largest measured 155 μ m

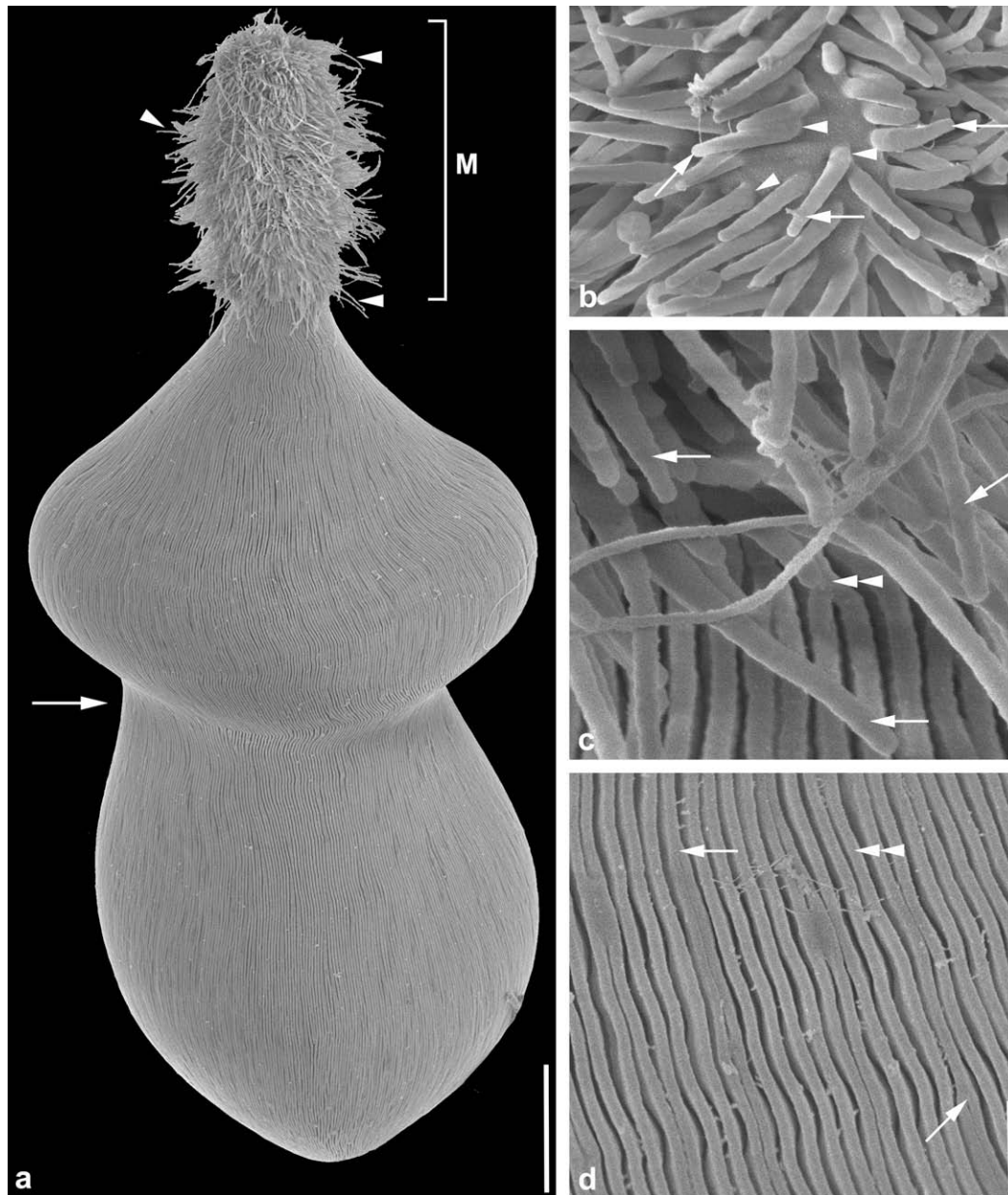
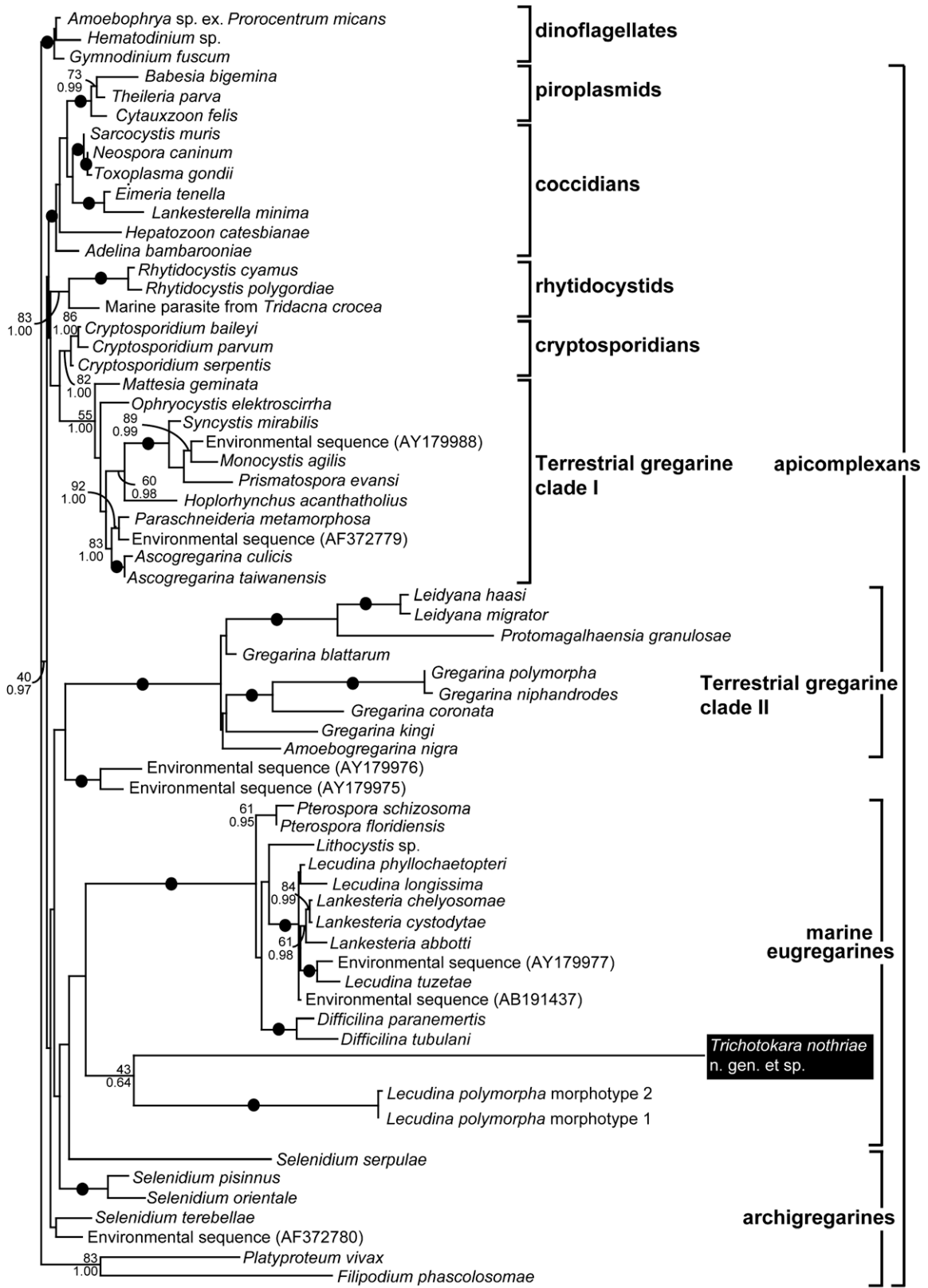


Fig. 2. Scanning electron micrographs (SEM) showing the general morphology and surface ultrastructure of *Trichotokara nothriae* n. gen. et sp. (a) SEM showing a trophozoite with an elongated mucron (M) covered in hair-like projections (arrowheads) of different lengths. The cell body proper has a transverse constriction in the middle of the cell (arrow), forming a posterior bulge and an anterior bulge. The trophozoite surface is inscribed by a densely packed arrangement of longitudinal epicytic folds. The posterior end is rounded. (b) High magnification SEM of the hair-like projections (arrow) protruding from the cell surface. Each projection stems from the cell cortex (arrowhead) rather than being attached to the surface. (c) High magnification SEM of the junction between the cell body proper and the elongated mucron. Hair-like projections (arrowheads) obscure the epicytic folds (double arrowhead) near the junction between the cell body proper and the mucron. (d) High magnification SEM of the densely packed longitudinal epicytic folds (double arrowhead). The arrows indicate epicytic folds that merge together. Scale bars: $a = 10 \mu\text{m}$; $b-d = 1.0 \mu\text{m}$.

long and $55 \mu\text{m}$ wide) (Table 1). *C. lysidice* and *C. emersoni* are dorsoventrally flattened with a sharply pointed posterior end (compare Hoshide, 1944, 1958; Levine, 1973); the trophozoites of *T. nothriae*, by contrast, lack both of these features and contain a prominent transverse constriction in the middle of the cell forming an anterior and posterior bulge. Moreover, hair-like projections on the mucron were not mentioned in the original descriptions of either the genus *Cochleomeritus* or *C. lysidice*, the type species (Hoshide, 1944, 1958). Levine (1973) also described wing-like extensions on the cell body proper of *C. emersoni* that curved over to form a longitudinal tube-like structure on the surface of the trophozoites; similar “wing-like” extensions along the longitudinal

axis were also indicated on the original line drawing of the type species, *C. lysidice* (Hoshide, 1944). The surface of the trophozoites of *T. nothriae* lacked any evidence of “wing-like” extensions and was inscribed with a densely packed arrangement of longitudinal epicytic folds. To summarize, the line drawings shown in the original descriptions of the two *Cochleomeritus* species are very similar to one another (Hoshide, 1944; Levine, 1973) and differ greatly from the LM and SEM micrographs of *T. nothriae*. Therefore, because the trophozoite morphology for *T. nothriae* did not conform to the diagnosis/description provided for the genus *Cochleomeritus* (Hoshide, 1944), we elected to establish a new genus name for the novel species described here.



Est. 0.1 substitutions/site

Fig. 3. Maximum-likelihood tree of apicomplexans (dinoflagellates = outgroup) as inferred using the GTR model of nucleotide substitutions, a gamma-distribution and invariable sites on an alignment of 64 SSU rDNA sequences and 1019 unambiguously aligned sites ($-\ln L = 13998.59297$, $\alpha = 0.450$, fraction of invariable sites = 0.068, eight rate categories). Numbers at the branches denote maximum likelihood (ML) bootstrap percentages (top) and Bayesian posterior probabilities (bottom). Black dots on branches denote Bayesian posterior probabilities of 0.95 or higher and ML bootstrap percentages of 95% or higher. The sequence addressed in this study is highlighted in the black box.

Table 1Summary of morphological characteristics observed in *Cochleomeritus lysidice*, *C. emersoni* and the newly described *Trichotokara nothriae* n. gen. et sp.

Host	<i>Cochleomeritus lysidice</i> (type species for the genus) <i>Lysidice punctata</i>	<i>Cochleomeritus emersoni</i> <i>Diopatra ornata</i>	<i>Trichotokara nothriae</i> n. gen. et sp. <i>Nothria conchylega</i>
Trophozoite morphology	Cell dorsoventrally flattened Spoon-shaped, widest part at anterior end Cell 520 µm long Cell 150 µm wide at the widest part Wing-like extensions along longitudinal axis No neck-like region at anterior end Pointed posterior end Nucleus in the anterior half to middle of the cell body Nucleus 30–40 µm in diameter	Cell dorsoventrally flattened Spoon-shaped, widest part at anterior end Cell 130–450 µm long Cell 23–175 µm wide at the widest part Folded wing-like extensions along longitudinal axis No neck-like region at anterior end Pointed posterior end Nucleus in anterior half of the cell body Nucleus 15–45 µm in diameter	Cell round in transverse section, not flattened Bulges at anterior and posterior end due to constriction in the middle of the cell body Cell 50–150 µm long Cell 14–55 µm wide at the widest part No wing-like extensions ~ 400 longitudinal epicytic folds Distinct neck-like region at anterior end Rounded posterior end Nucleus in the middle of the cell body or slightly shifted anterior or posterior Nucleus 8–20 µm in diameter
Mucron	Club shaped, pointed like a pin, elastic 20 µm long No hair-like projections on mucron	Variable in shape, mostly cylindrical 18–67 µm long 8–26 µm wide Coarse hairs along all or part of the length of the mucron	Cylindrical 14–60 µm long 6–12 µm wide Hair-like projections covering the entire length of the mucron

The new SSU rDNA sequence from *T. nothriae* is the first available molecular phylogenetic data from marine eugregarines that possess hair-like surface projections. The trophozoites of other gregarines, like species of *Filipodium*, also possess hair-like projections that are similar to those in *T. nothriae*, making the phylogenetic distribution of this character difficult to interpret from morphology alone (Hoshida and Todd, 1996). This issue is reflected in the historically unstable systematic position of *Filipodium* (Rueckert and Leander, 2009): *Filipodium* was first placed within the septate gregarine family Dactylophoridae (Hukui, 1939), later moved to the aseptate family Lecudinidae (Grassé, 1953), and on the basis of similar hair-like projects, could be considered closely related to *T. nothriae*. Molecular phylogenetic analyses, however, demonstrate that *Filipodium*, specifically *F. phascolosomae*, is actually an archigregarine, more closely related to lineages like *Selenidium* and *Platyproteum*, and only distantly related to *T. nothriae* (Rueckert and Leander, 2009; Fig. 3). This molecular phylogenetic context indicates that the possession of hair-like projections has evolved convergently in several different lineages of gregarines and that a combination of morphological and molecular phylogenetic data is critical for understanding the systematics and character evolution of the group.

The molecular phylogenetic analyses also demonstrated that the SSU rDNA sequence from *T. nothriae* clustered with sequences from two morphotypes of *L. polymorpha* (Fig. 3), the only other SSU rDNA sequences from lecutinid gregarines that possess a prominently elongated mucron (Leander et al., 2003b). Like the sequences from *T. nothriae*, the sequences from the two morphotypes of *L. polymorpha* were highly divergent relative to the other known gregarine sequences. Because these three distinctive sequences cluster in a clade that forms the sister group to the clade consisting of all other marine eugregarines (e.g., *Pterospora*, *Lithocystis*, *Lankesteria*, *Difficilina*, and *Lecudina*), we question whether *L. polymorpha* should be considered a member of the genus *Lecudina*. The type species of *Lecudina*, namely *Lecudina pelucida*, possesses the same basic trophozoite morphology described for *L. tuzetae* (Schrével, 1969; Vivier, 1968; Leander et al., 2003b), which is deeply nested within the main marine eugregarine clade and only distantly related to the *L. polymorpha* sequences (Fig. 3). This molecular phylogenetic context and the shared morphological features with *T. nothriae* (i.e., the elongated mucron and densely packed epicytic folds) indicate that *L. polymorpha* should probably

be removed from *Lecudina* and re-classified within a different genus.

Nonetheless, the precise phylogenetic positions of *T. nothriae* and *L. polymorpha* within marine eugregarines remain unclear, mainly because of the limited taxon sample and because the sequences from these species are among the most divergent of all known sequences from gregarines. The limited number of gregarine sequences available in GenBank makes it especially difficult to identify new highly divergent sequences by BLAST analysis alone, and for this reason, we evaluated the sequences from *T. nothriae* and *L. polymorpha* within the context of a 42-taxon alignment representing all major groups of eukaryotes (Supplementary file). The phylogenetic relationships and systematics of marine gregarine is expected to become much more robust as molecular sequence data from these lineages continues to accumulate. Ideally, molecular phylogenetic analyses using several different molecular markers (e.g., large subunit rDNA, heat shock protein 90 and actin) will become more feasible and ultimately help resolve the deepest relationships among gregarines and apicomplexans as a whole.

5. Taxonomic summary

Phylum: Myzozoa Cavalier-Smith and Chao, 2004
Subphylum: Apicomplexa Levine, 1970
Order: Eugregarinorida Léger, 1900
Family: Lecudinidae Kamm, 1922

5.1. Genus *Trichotokara* n. gen. Rueckert and Leander

Diagnosis: Trophozoites with a dense distribution of longitudinal epicytic folds (about 5 folds/µm); mucron covered in hair-like projections; body proper not dorsoventrally flattened; posterior end rounded; either non-motile or gliding motility; in the intestines of polychaetes.

Type species: *Trichotokara nothriae*.

Etymology: The generic name stems from the greek adjective *trichotos* which means hairy and the noun *kara*, which means head or top (compare Brown, 1956). The gender of the name is neuter. The name refers to the mucron that is covered in hair-like projections.

Remarks: Until now, no gregarine species have been described from the polychaete host *N. conchylega*. Even though *C. emersoni* was also described from an onuphid polychaete and has hairs on the mucron (Levine, 1973), these hairs were not mentioned in the original description of the genus or its type species (Hoshide, 1958; Levine, 1973). Moreover, the overall shape and morphology of the trophozoites within the *Cochleomeritus* genus (e.g., dorso-ventrally flattened, lateral wings) differ substantially from the trophozoites of the new species described here; this prompted us to establish a new genus.

5.2. *Trichotokara nothriae* n. sp. Rueckert and Leander

Description: Trophozoites about 93 µm long (50–155 µm, $n = 23$) with a guitar-like shape. Cells not flattened but round in transverse section. Cells rigid and non-motile. Trophozoite surface inscribed by approximately 400 longitudinal epicytic folds (5 folds/µm). Mucron free of folds, covered in hair-like projections that protrude from the cell surface. Transverse constriction in the middle of the trophozoite that forms two prominent bulges: anterior bulge 28 (14–48) µm wide; posterior bulge 30 (15–55) µm wide. Posterior end of cell body rounded to pointed. Anterior end of cell body tapered into a neck-like constriction before joining the mucron. Mucron 31 µm long (14–60 µm, $n = 24$) and 10 µm (6–12 µm, $n = 24$) wide, covered with hair-like projections 1.97 µm (0.77–4.3 µm, $n = 11$) long and 0.2 µm (0.18–0.23 µm, $n = 11$) wide at the base. Mucron can be absent. A thin prolongation of the cell body forms the core of the mucron. Spherical nucleus 12 (8–20) µm in diameter ($n = 19$) situated in the middle of cell body proper. Nucleolus 4 µm in diameter. Cytoplasm granular, brownish in colour. Gamonts with end-to-end syzygy, without mucron. Neither sporozoites nor oocysts were observed.

Iconotype: Figs. 1a and 2a.

Hapantotype: Parasites on gold sputter-coated SEM stubs have been deposited in the Beaty Biodiversity Museum (Marine Invertebrate Collection) at the University of British Columbia, Vancouver, Canada.

Type host: *Nothria conchylega* (Sars, 1835) (Metazoa, Annelida, Polychaeta, Onuphidae).

Type locality: Wizard Islet (48°51'6"N, 125°09'4"W) near Bamfield Marine Sciences Centre, Vancouver Island, Canada; shelly gravel sediment at a depth of 20 m.

Habitat of the host: Marine.

Site of infection: Intestinal lumen.

Etymology: The species name *nothriae* refers to the genus of the polychaete type host *N. conchylega* (Sars, 1835).

Gene sequence: The partial SSU rDNA sequence of the gregarine, *T. nothriae* has been deposited in the GenBank database under Accession number GU592817.

Acknowledgments

The authors would like to thank the crew of MV/Alta for their help in collecting the specimens of *N. conchylega* and Tara McDonald for the identification of the polychaete host. This work was supported by grants from the Tula Foundation (Centre for Microbial Diversity and Evolution), the National Science and Engineering Research Council of Canada (NSERC 283091-09) and the Canadian Institute for Advanced Research, Program in Integrated Microbial Biodiversity.

Appendix A. Supplementary data

Supplementary data associated with this article can be found, in the online version, at doi:10.1016/j.jip.2010.03.005.

References

- Adl, S., Simpson, A.G.B., et al., 2005. The new higher level classification of eukaryotes with emphasis on the taxonomy of protists. *J. Eukaryot. Microbiol.* 52, 399–451.
- Adl, S., Leander, B.S., Simpson, A.G.B., et al., 2007. Diversity, nomenclature, and taxonomy of protists. *Syst. Biol.* 56, 684–689.
- Brown, R.W., 1956. *Composition of Scientific Words*. Smithsonian Books, Washington, DC.
- Dyakin, A.Yu., Simdyanov, T.G., 2005. The cortical zone of skittle-like cells of *Urospora chiridotae*, a gregarine from an apode holothuria *Chiridota laevis*. *Protistology* 4, 97–105.
- Grassé, P.-P., 1953. Classe des grégarinomorpes (Gregarinomorpha, *N. nov.*, Gregarinae Haeckel, 1866; gregarinidea Lankester, 1885; grégarines des auteurs). In: Grassé, P.-P. (Ed.), *Traité de Zoologie*. Masson, Paris, pp. 590–690.
- Guindon, S., Gascuel, O., 2003. A simple, fast, and accurate algorithm to estimate large phylogenies by maximum likelihood. *Syst. Biol.* 52, 696–704.
- Guindon, S., Lethiec, F., Duroux, P., Gascuel, O., 2005. PHYML online – a web server for fast maximum likelihood-based phylogenetic inference. *Nucleic Acids Res.* 1, 33.
- Hausmann, K., Hülsmann, N., Radek, R., 2003. *Protistology*, third compl. rev. ed. E. Schweizerbart'sche Verlagsbuchhandlung, Stuttgart.
- Hoshide, H., 1944. Studies on eugregarines from polychaetes in Japan. *J. Sci. Hiroshima Univ., Ser. B, Div. 1* (10), 213–235.
- Hoshide, H., 1958. Studies on the cephaline gregarines of Japan (II). *Bull. Fac. Educ., Yamaguchi Univ.* 6, 97–157.
- Hoshide, H., Todd Jr., K.S., 1996. The fine structure of cell surface and hair-like projections of *Filipodium ozakii* Hukui 1939 gamonts. *Acta Protozool.* 35, 309–315.
- Huelsenbeck, J.P., Ronquist, F., 2001. MrBayes: Bayesian inference of phylogenetic trees. *Bioinformatics* 17, 754–755.
- Hukui, T., 1939. On the gregarines from *Siphonosoma cumanense* (Keferstein). *J. Sci. Hiroshima Univ.* 7, 1–23.
- Landers, S.C., Leander, B.S., 2005. Comparative surface morphology of marine coelomic gregarines (Apicomplexa, Urosporidae): *Pterospora floridiensis* and *Pterospora schizosoma*. *J. Eukaryot. Microbiol.* 52, 23–30.
- Leander, B.S., 2008. Marine gregarines – evolutionary prelude to the apicomplexan radiation? *Trends Parasitol.* 24, 60–67.
- Leander, B.S., Saldarriaga, J.F., Keeling, P.J., 2002. Surface morphology of the marine parasite *Haplozoon axiothellae* (Dinoflagellata). *Eur. J. Protistol.* 38, 287–298.
- Leander, B.S., Clopton, R.E., Keeling, P.J., 2003a. Phylogeny of gregarines (Apicomplexa) as inferred from small-subunit rDNA and beta-tubulin. *Int. J. Syst. Evol. Microbiol.* 53, 345–354.
- Leander, B.S., Harper, J.T., Keeling, P.J., 2003b. Molecular phylogeny and surface morphology of marine aseptate gregarines (Apicomplexa): *Selenidium* and *Lecudina*. *J. Parasitol.* 89, 1191–1205.
- Levine, N.D., 1973. *Cochleomeritus emersoni* sp. n. (Protozoa, Apicomplexa), a lecudinid gregarine from the Pacific Ocean polychaete *Diopatra ornata* Moore, 1911. *J. Protozool.* 20 (5), 546–548.
- Levine, N.D., 1976. Revision and checklist of the species of the aseptate gregarine genus *Lecudina*. *Trans. Am. Microsc. Soc.* 95, 695–702.
- Levine, N.D., 1977. Revision and checklist of the species (other than *Lecudina*) of the aseptate gregarine family Lecudinidae. *J. Protozool.* 24, 41–52.
- Levine, N.D., 1979. New genera and higher taxa of septate gregarines (Protozoa, Apicomplexa). *J. Protozool.* 26, 532–536.
- Levine, N.D., 1988. Progress in taxonomy of the apicomplexan protozoa. *J. Protozool.* 35, 518–520.
- Maddison, D.R., Maddison, W.P., 2000. *MacClade 4*. Sinauer Associates, Sunderland.
- Morrison, D.A., 2009. Evolution of the Apicomplexa: where are we now? *Trends Parasitol.* 25, 375–382.
- Perkins, F.O., Barta, J.R., Clopton, R.E., Pierce, M.A., Upton, S.J., 2000. Phylum Apicomplexa. In: Lee, J.J., Leedale, G.F., Bradbury, P. (Eds.), *The Illustrated Guide to the Protozoa*. Allen Press, Inc., Lawrence, pp. 190–304.
- Posada, D., Crandall, K.A., 1998. MODELTEST: testing the mode I of DNA substitution. *Bioinformatics* 14, 817–818.
- Prensier, G., Dubremetz, J.-F., Schrével, J., 2008. The unique adaptation of the life cycle of the coelomic gregarine *Diplauxis hattii* to its host *Perinereis cultrifera* (Annelida, Polychaeta): an experimental and ultrastructural study. *J. Eukaryot. Microbiol.* 55, 541–553.
- Rueckert, S., Leander, B.S., 2008. Morphology and molecular phylogeny of *Haplozoon praxillellae* n. sp. (Dinoflagellata): a novel intestinal parasite of the maldanid polychaete *Praxillella pacifica* Berkeley. *Eur. J. Protistol.* 44, 299–307.
- Rueckert, S., Leander, B.S., 2009. Molecular phylogeny and surface morphology of marine “archigregarines” (Apicomplexa) – *Selenidium* spp., *Filipodium phascosomae* n. sp. and *Platyproteum* n. gen. et comb. – from North-eastern Pacific peanut worms (Sipuncula). *J. Eukaryot. Microbiol.* 56, 428–439.
- Schrével, J., 1969. Recherches sur le cycle des Lecudinidae grégarines parasites d'Annélides Polychètes. *Protistologica* 5, 561–588.
- Simdyanov, T.G., 2009. *Difficilina cerebratulii* gen. n., sp. n. (Eugregarinida: Lecudinidae) – a new gregarine species from the nemertean *Cerebratulus barentsi* Bürger, 1895 (Nemertini: Cerebratulidae). *Parazitologiya* 43, 273–287.
- Vivier, E., 1968. L'organisation ultrastructurale corticale de la gregarine *Lecudina pellucida*: ses rapports avec l'alimentation et la locomotion. *J. Protozool.* 15, 230–245.